Protein Science (1999), *8*:1954–1961. Cambridge University Press. Printed in the USA.

Solution structure of the receptor tyrosine kinase EphB2 SAM domain and identification of two distinct homotypic interaction sites

MAIKA SMALLA,[1] PETER SCHMIEDER,[1] MARK KELLY,[1] ANTONIUS TER LAAK,[1] GERD KRAUSE,[1] LINDA BALL,[1] MARTIN WAHL,[1] PEER BORK,[2] AND HARTMUT OSCHKINAT[1]

[1]Forschungsinstitut für Molekulare Pharmakologie, Alfred-Kowalke-Str. 4, D-10315 Berlin-Friedrichsfelde, Germany
[2]European Molecular Biology Laboratory, Meyerhofstraße 1, D-69117 Heidelberg, Germany

(RECEIVED March 12, 1999; ACCEPTED June 18, 1999)

Abstract

The sterile alpha motif (SAM) is a protein interaction domain of around 70 amino acids present predominantly in the N- and C-termini of more than 60 diverse proteins that participate in signal transduction and transcriptional repression. SAM domains have been shown to homo- and hetero-oligomerize and to mediate specific protein–protein interactions. A highly conserved subclass of SAM domains is present at the intracellular C-terminus of more than 40 Eph receptor tyrosine kinases that are involved in the control of axonal pathfinding upon ephrin-induced oligomerization and activation in the event of cell–cell contacts. These SAM domains appear to participate in downstream signaling events via interactions with cytosolic proteins.

We determined the solution structure of the EphB2 receptor SAM domain and studied its association behavior. The structure consists of five helices forming a compact structure without binding pockets or exposed conserved aromatic residues. Concentration-dependent chemical shift changes of NMR signals reveal two distinct well-separated areas on the domains' surface sensitive to the formation of homotypic oligomers in solution. These findings are supported by analytical ultracentrifugation studies. The conserved Tyr932, which was reported to be essential for the interaction with SH2 domains after phosphorylation, is buried in the hydrophobic core of the structure.

The weak capability of the isolated EphB2 receptor SAM domain to form oligomers is supposed to be relevant in vivo when the driving force of ligand binding induces receptor oligomerization. A formation of SAM tetramers is thought to provide an appropriate contact area for the binding of a low-molecular-weight phosphotyrosine phosphatase and to initiate further downstream responses.

Keywords: Eph receptor; oligomerization; SAM domain; tyrosine phosphorylation

The sterile alpha motif (SAM) domain is a novel protein module of around 70 amino acids originally found in a set of developmental proteins, like Ste4 and Byr2, and polyhomeotic proteins (Ponting, 1995). Later, its systematic appearance as a highly conserved domain at the C-terminus of Eph-family receptor tyrosine kinases was detected, suggesting an important role in cell–cell contacts and signaling processes (Schultz et al., 1997). Furthermore, a tumor suppressor protein, p73, was found to differ from the homologue p53 by an additional C-terminal SAM domain (Bork & Koonin, 1998). It was proposed that SAM domains may mediate protein–protein contacts, yet the molecular mechanisms employed in vivo are still unclear. Self-association of SAM domains may be considered, as suggested by data from yeast two-hybrid experiments on the yeast sex development proteins Ste4 and Byr2 (Barr et al., 1996), and on proteins of the polyhomeotic family (Kyba & Brock, 1998). SAM-SH2 interactions may also be relevant, since phosphorylation of a tyrosine in the SAM domain of the EphB1 receptor lead to the subsequent binding of Grb10 (Stein et al., 1996).

Receptor tyrosine kinases of the Eph family (Eph Nomenclature Committee, 1997) are involved in contact-mediated axon guidance, axon fasciculation, vascular network assembly, capillary

Reprint requests to: Dr. Hartmut Oschkinat, Forschungsinstitut für Molekulare Pharmakologie, Alfred-Kowalke-Str. 4, D-10315 Berlin-Friedrichsfelde, Germany; e-mail: Oschkinat@fmp-berlin.de.

Abbreviations: DIPSI, decoupling in the presence of scalar interactions; DQF-COSY, double quantum filtered correlation spectroscopy; Eph receptor, a receptor named for its expression in an erythropoietin-producing human hepatocellular carcinoma cell line; HSQC, heteronuclear single quantum coherence; IPTG, isopropyl-β-D-thiogalactopyronoside; LMW-PTP, low-molecular-weight phosphotyrosine phosphatase; NMR, nuclear magnetic resonance; NOE, nuclear Overhauser effect; NOESY, NOE spectroscopy; MEXICO, measurement of exchange rates in isotopically labeled compounds; PCR, polymerase chain reaction; PMSF, phenylmethylsulfonylfluoride; SDS-PAGE, sodium dodecyl sulfate–polyacrylamide gel electrophoresis; RMSD, root-mean-square deviation; TOCSY, total correlation spectroscopy.

morphogenesis, and angiogenesis. They are activated upon oligomerization and binding of their extracellular ligands, the ephrins (Orioli & Klein, 1997), which may themselves act as receptors, mediate bidirectional signaling in the event of cell–cell contacts (Holland et al., 1996; Brückner et al., 1997). Upon ligand-induced receptor dimerization, tyrosine phosphorylation at intracellular sites on the receptor subunits occurs (Davis et al., 1994). However, a more complex behavior, involving differential functions of higher order receptor oligomers, was also observed (Stein et al., 1998). In particular, it was shown that only activated receptor tetramers are able to bind a low-molecular-weight phosphotyrosine phosphatase (LMW-PTP) and to initiate a hitherto different cellular attachment response than the dimeric form. The formation of oligomers has also been discussed on the basis of two recent Eph receptor SAM domain X-ray structures (Stapleton et al., 1999; Thanos et al., 1999), pointing out important N- and C-terminal interactions.

We have determined the structure of the SAM domain from the receptor tyrosine kinase EphB2 in solution. Studies of the hydrodynamic properties of the SAM domain and the concentration dependence of chemical shifts identified by NMR give evidence for its ability to self-associate specifically as isolated domain in solution with low affinity. The results indicate a possible involvement of SAM domains in receptor clustering.

Results

Structure determination

We determined the solution structure of the SAM domain from the tyrosine kinase receptor EphB2. Two C-terminally differing His_6-tagged constructs containing the EphB2 receptor SAM domain (Fig. 1, bottom) were expressed and purified. Construct 1 consisted of a domain confined by sequence alignment; the other contained the additional six remaining C-terminal residues of the EphB2 receptor C-terminus. Attempts to express shorter constructs were not successful. Both constructs were investigated by analytical ultracentrifugation under the same conditions and their behavior was identical. Construct 1 was uniformly labeled with $^{15}N/^{13}C$ and forms a stable and folded domain in solution. Heteronuclear multidimensional NMR experiments (Clore & Gronenborn, 1991) were performed and a complete assignment of proton, carbon, and nitrogen resonances was obtained. Structures were calculated based on 1,291 distance constraints from two- and three-dimensional NOESY spectra.

Description of the structure

The structure consists of four α-helices and one short 3_{10} helix whose hydrophobic faces form the compact hydrophobic core of the protein (Fig. 2A,B) (Table 1). The domains' surface is relatively smooth, without pronounced gorges or binding pockets. The helices are connected by well-defined loops that do not adopt a variety of conformations (Fig. 2A; Table 1). The N- and C-termini are close together in the structure, with Tyr7 and Asn74 defining the domain boundaries. The hydrophobic core is made up by the residues Val13, Trp16, Leu17, Ile20, Met22, Tyr25, Phe29, Phe34, Val40, Met43, Ile48, Val51, Val53, His58, Ile62, Ile66, and Met69, in which the hydroxyl of Tyr25 and His58 are involved in a hydrogen bond covered by Leu55 (see Figs. 1, 2B, green residues). A major role for the fold is probably played by the highly conserved Trp16, which is nearly completely buried, and which is involved in contacts with Leu17, Ile20, Phe29, Val40, and Met69. Its side chain NH is pointing toward the conserved Ser65. A number of hydrophobic residues, namely Ile39, Val45, Leu49, Leu55, and Leu63, are found exposed on the surface of the protein. However, the surface seems to be rather hydrophilic. Most of the charged residues are distributed evenly, except for Lys21, Lys60, and Lys61, which are in close proximity to His58, at the beginning of the helices 2 and 5. Interestingly, a number of hydrophilic residues on the surface show strong homology within 32 sequences of the Eph receptor family. The residues Thr12, Glu15, Lys21, Thr36, Asp38, Glu46, Asp47, Gln59, Lys60, Lys61, Ser65, and Arg70 are conserved to more than 90%, when only Asp/Glu, Arg/Lys, or Thr/Ser substitutions are taken into consideration, except for Lys60, for which also Asn appears frequently.

Analysis of the topology

A search through the Protein Data Bank (PDB) database for homologous structures was performed using the topology analysis programs SCOP (Murzin et al., 1995) and DALI (Holm & Sander, 1993). The topology of the SAM domain was observed as a substructure in three protein families, these comprising a set of proteins involved in DNA recombination and repair (RuvA, 1cuk) (Rafferty et al., 1996), endo nuclease III, which is also involved in DNA repair (2abk) (Kuo et al., 1992), and DNA polymerase β (1bpd) (Sawaya et al., 1994). The conserved structural elements deviated from our lowest energy structure by root-mean-square deviation (RMSD) values (Cα) of 3.0, 2.7, and 3.1 Å, respectively. In two cases (1cuk and 2abk), the interface with the other subunits of the respective proteins was formed by a hydrophobic surface made up by helices 1 and 2. The hydrophobic residues that mediate these contacts are indicated below the respective sequences in Figure 1. The DNA polymerase β (1bpd) contains a SAM-like substructure (lacking helix 4) as a module/domain that was attached to the rest of the protein by a linker peptide. There are, however, contacts between its C-terminal helix and a symmetry-related molecule. All these proteins were not detected in sequence profile searches of SAM, probably due to the presence of the hydrophobic patches on the surface of the other proteins, and the inclusion of hydrophilic constraints at the same sites in the search profile. The interactions observed in these proteins are examples for potential protein–protein contacts in which SAM domains might be involved.

Tyrosine phosphorylation

It has been reported for the EphB1 receptor SAM domain that the homologue of our Tyr25, i.e., Tyr929 in EphB1, becomes phosphorylated upon ephrin-dependent activation (Stein et al., 1996). The structure shows this tyrosine to be located in the interior of the protein (Fig. 2A,B), involved in a hydrogen bond with His58. Neither the signal of the Tyr25 nor the signal of the His58 exhibited chemical shift changes at different pH values. Phosphorylation of Tyr25 would require a structural change for this residue to become exposed on the surface. In this context, attempts to phosphorylate our domain with src-kinase were not successful (K. Kullander & R. Klein, pers. comm.) The area around Tyr25 (Tyr932 in EphB2 receptor) is well ordered, hence the possibility of phosphorylation facilitated by an inherent flexibility of the structure can be excluded.

Fig. 1. Sequence alignment, including SAM domains within Eph receptors (first block), proteins from the polyhomeotic family (second block), the yeast sex development proteins Byr2 and Ste4 (third block), the p73 sequence, the three sequences of proteins whose structures contain SAM-like substructures, i.e., the RuvA protein (1cuk), polymerase β of rats (1bpd), and endonuclease III (2abk), and of the constructs made for this investigation. The positions of the helices are indicated by rectangles above the first sequence, and for sequences of the SAM-like substructures of the three proteins found by DALI. Green columns indicate internally oriented hydrophobic residues. The residues Y932 (Y25 in construct 1) and H965 (H58 in construct 1) that are highly conserved in Eph receptor SAM domains are highlighted in violet and cyan. Those residues that may support self-association of SAM domains of the polyhomeotic family are indicated by a yellow background. Above the polyhomeotic sequence (first entry in block 2), the mutations that abolish positive answers in two-hybrid experiments are shown. Residues that are solvent-exposed in the solution structure are indicated with an ampersand (&) on top of the figure. Below the last three sequences, residues indicated with # are involved in contacts between the SAM-like substructure and the other sites of the respective protein. Below the alignment, protein association sites are indicated by + (area 1) and ^ (area 2). The numbering on top of the alignment is valid for the EphB2 receptor; the numbering above construct 1 is used in this paper.

Homo- and hetero-oligomerization

Studies employing the yeast two-hybrid system showed the ability of SAM domains to form homo- or heterologous oligomers (Barr et al., 1996; Kyba & Brock, 1998). In particular, the proteins Ste4 and Byr2 show a tendency to associate that was assigned to interactions of their SAM domains (Barr et al., 1996). In a study employing isolated SAM domains of proteins from the polyhomeotic family (ph) self-association was observed, and the domains of ph, Scm, and RAE 28 showed heterologous interactions (Kyba & Brock, 1998). These effects are probably mediated largely by interactions between hydrophobic surfaces of the domain. The sequences of the polyhomeotic family indeed exhibit a number of additional conserved hydrophobic residues in positions 39, 47, 58, 59, and 60 (Fig. 1, construct 1, yellow columns in second block). The importance of positions 39 and 47 was demonstrated by the appropriate mutations (Kyba & Brock, 1998) (Fig. 1, above the polyhomeotic sequence).

Since SAM–SAM interactions in Eph receptor systems would be promoted by ephrin-induced oligomerization, the formation of homo-oligomers by Eph receptor SAM domains is plausible. Its oligomerization can also be postulated based on the observation that an LMW-PTP binds to the C-terminal SAM domain after tetramer formation of the receptor system (Stein et al., 1998). However, only a modest tendency for self-association of the isolated SAM domain would be required when receptor tetramer for-

Table 1. *Structure statistics of the ensemble of 10 SAM structures*

Constraints for structure calculations	
Total constraints used	1,319
Total NOE constraints	1,291
Intraresidue	611
Sequential ($\|i - j\| = 1$)	280
Medium range ($1 < \|i - j\| \leq 4$)	207
Long range ($\|i - j\| > 4$)	193
Hydrogen bond constraints	28
Statistics of structure calculations	⟨SA⟩[a]
Final energies (kcal/mol)	
E_{total}	110.8 ± 2.3
E_{bonds}	2.5 ± 0.2
E_{angles}	76.4 ± 0.9
$E_{impropers}$	9.1 ± 0.1
E_{vdW}	5.2 ± 0.8
E_{NOE}	17.6 ± 1.8
NMR constraint violations	
Number of NOE constraint violations > 0.3 Å in 10 structures[a]	17
Number of NOE constraint violations > 0.5 Å in 10 structures[a]	4
Coordinate precision[b] (Å)	
RMSD of backbone atoms (N,Cα,C′) 7–74	0.37 ± 0.07
RMSD of all heavy atoms 7–74	0.74 ± 0.07
Ramachandran statistics for residues 7–74[c]	
Residues in the most favored regions	72.2%
Residues in additional allowed regions	26.0%
Residues in generously allowed regions	1.6%
Residues in disallowed regions	0.2%

[a] ⟨SA⟩ refers to the ensemble of the 10 structures with the lowest energy from 200 calculated structures.

[b] RMSD between the ensemble of structures ⟨SA⟩ and the average structure of the ensemble ⟨SA⟩.

[c] The program PROCHECK (Laskowski et al., 1993) was used to assess the overall quality of the structures.

mation is ligand induced. To support this hypothesis, we have investigated the self-association behavior of our SAM domain by measuring its sedimentation behavior in an analytical ultracentrifuge, by applying the two-hybrid system to the isolated domain, by measuring relaxation parameters of the NMR signals, and by monitoring ^{1}H and ^{15}N chemical shift changes in a concentration-dependent manner.

At first, construct 1 was investigated by analytical ultracentrifugation at protein concentrations of 80 μM and 1.6 mM EphB2-SAM. At the lower concentration, the result of the measurement is in agreement with a monodisperse monomeric solution. Fitting of the sedimentation equilibrium data obtained at the higher concentration to a monomer-dimer-tetramer equilibrium model resulted in small residual deviations. In contrast, fitting with a monomer and monomer-dimer equilibrium model increased the deviations significantly. To investigate the possible influence of the six C-terminal residues following the SAM domain, construct 2 was also investigated under the same conditions. Its behavior was identical to that of construct 1.

Attempts to observe homotypic interactions between our EphB2 SAM domain using the two-hybrid system did not produce positive signals (R. Poppe, pers. comm.). Interestingly, the largely hydrophilic surface of our EphB2 domain shows a relatively small number of exposed hydrophobic residues in comparison with the sequences of the polyhomeotic SAM domains (Fig. 1, yellow columns).

The overall correlation time was estimated by NMR spectroscopy. At low concentration (200 μM) the correlation time was 5 ns, as expected for a monomer. It increased only slightly to 6 ns at a concentration of 1.6 mM, indicating the beginning of an association process. When the protein concentration was raised to 3.0 mM, the correlation time increased to 12.5 ns.

The dependency of the chemical shifts on the protein concentration was then studied in solution by ^{1}H-^{15}N-HSQC NMR spectroscopy to monitor the weak but specific association processes. Residue-specific chemical shift changes were observed when the concentration of the NMR sample was varied from 1.5 to 3.0 mM of protein. The residues showing the strongest chemical shift changes were Tyr7, Thr8, Phe10, Ala32, Asp38, Ile39, Val40, Asp47, Leu55, Ala56, Gly57, His58, Lys60, Lys61, Met69, and Met73. Other residues showed much smaller effects, where Ser9, Asn11, Trp16, Leu17, Gln24, Ser31, Ser41, Gln42, Met43, Leu49, Arg50, Val51, Val53, Ile66, Arg70, Gln72, Asn74, and Gln75 still displayed intermediate responses. The residues Thr12, Gln15, Asp18, Ala19, Ile20, Lys21, Met22, Ser23, Tyr25, Lys26, Glu27, Ser28, Ala30, and Leu63 remained unchanged. We conclude from these data that specific association occurs, but with low affinity.

The residues showing the strongest chemical shift changes are on two opposite faces of the structure. The locations of affected residues are shown in Figure 2C by means of partial Conolly surfaces made up by the residues with the strongest responses. The residues in helices 1 and 2 on the front of the view in Figure 2C exhibit only minor chemical shift changes. Interestingly, the charged residues that are highly conserved within the Eph receptor SAM domain family are located in or around the Conolly surface areas shown in Figure 2C.

Discussion

Our results suggest a role of the Eph receptor SAM domains in oligomerization processes induced by ligand binding. The residues showing large chemical shift changes upon variation of the protein concentration are located on two distinct surface areas demonstrating specific SAM–SAM interactions. The identification of these two distinct protein interaction sites on opposite sides of the domains' surface is not compatible with EphB2 SAM dimerization without major changes to the protein fold. Furthermore, results from analytical ultracentrifugation studies satisfy a monomer-dimer-tetramer equilibrium, but not a monomer-dimer equilibrium. These data are in line with the observations made by Stein et al. (1998), who found that higher-order clustering of Eph receptors is necessary for recruiting LMW-PTP to the receptor complex, and for achieving certain cellular responses. As was demonstrated by using isolated Fc-linked Ephrin dimers and tetramers, the binding of LMW-PTP to EphB1 receptors can only be induced by activation through tetramers, not dimers.

The formation of higher-order oligomers of EphB2 domains is also known from a recently solved X-ray structure (Thanos et al., 1999). This X-ray structure contains two types of monomers that have largely extended N-termini, suggested to be involved in oligomeric contacts. Interestingly, the SAM structure in solution clearly differs from the crystal structure at the N-terminus, exactly where

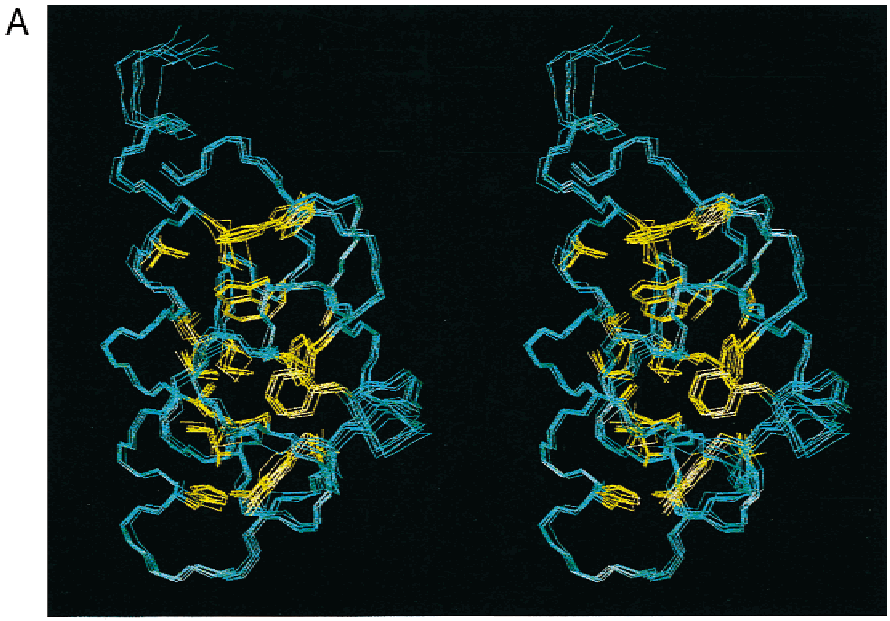
A

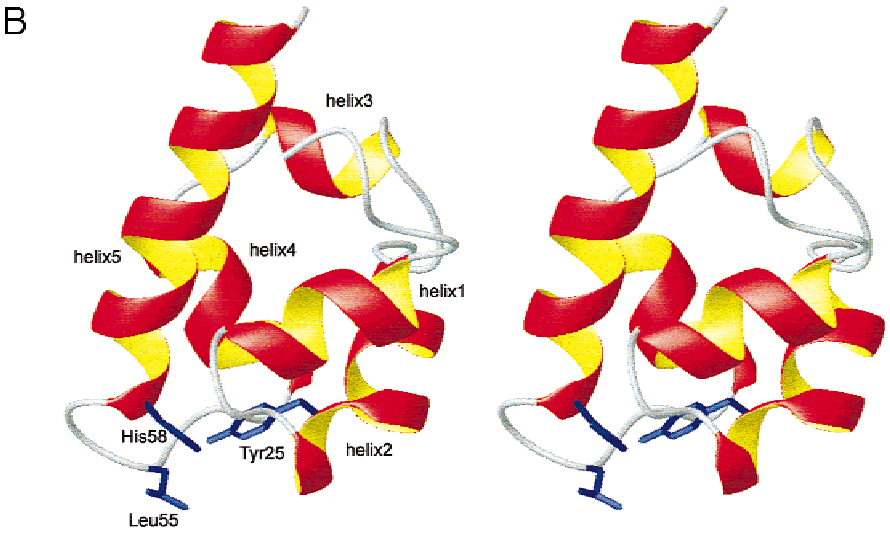
B
helix3
helix5
helix4
helix1
His58
Tyr25
helix2
Leu55

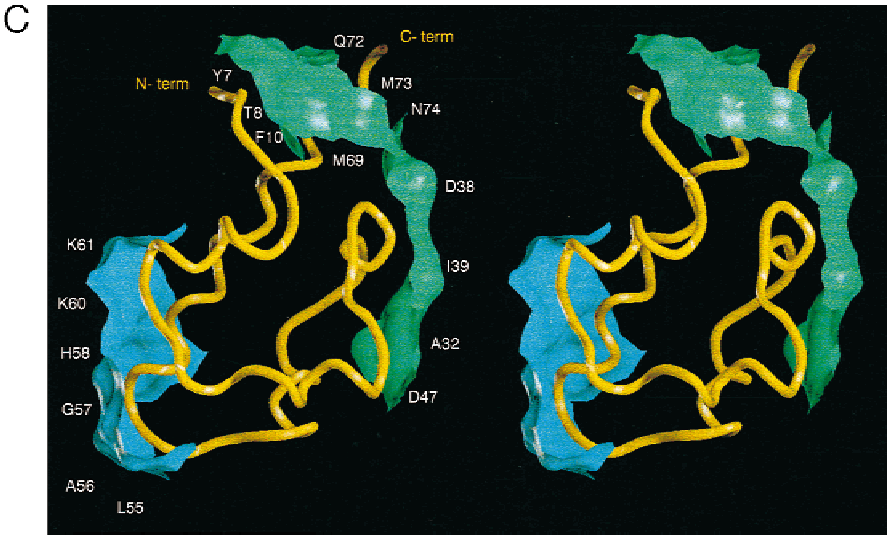
C
Q72
C- term
N- term
Y7
M73
T8
N74
F10
M69
D38
K61
I39
K60
H58
A32
G57
D47
A56
L55

Table 2. *Comparison of the NMR structure with X-ray structures*

X-ray structures	SAM EphB2(A)	SAM EphB2(B)	SAM EphA4
RMSD secondary structure[a]	1.27 ± 0.07	1.11 ± 0.06	1.36 ± 0.07
RMSD residues 12–73[a]	1.50 ± 0.06	1.35 ± 0.05	1.62 ± 0.06

[a] RMSD of X-ray structures (Stapleton et al., 1999; Thanos et al., 1999) relative to the backbone atoms (N,Cα,C′) of the NMR ensemble ($N = 10$).

chemical shift changes at higher protein concentrations indicate protein–protein interactions (Fig. 2C, area 1; Fig. 3). The globular fold of the SAM domain's five helices is still similar in the crystal and in solution as shown by the RMSD values in Table 2. In the monomeric solution structure, the N- and C-termini are close together and show important hydrophobic contacts between Tyr7 and Val68, Met69, and Met73 of helix 5. The presence of these NOEs at a low protein concentration of 100 μM confirms the closed monomer structure in solution. In the crystal structure, however, Tyr7 of a monomeric unit is clearly exposed. A possible explanation is that the EphB2 SAM domain switches from a closed monomeric state to an extended form upon oligomerization whereby a binding pocket arises at the place where Tyr7 was located. In a concerted manner, the now extended N-terminus would be able to interact with the arising interface of the pocket in another monomer. In particular, the X-ray structure shows that Tyr7 of the extended N-terminus fits into an adjacent binding pocket made up by Phe10, Trp16, Phe37, Val68, and Met69. Furthermore, the EphB2 SAM crystal structure displays a second interface where the residues Met44, Met45 (Thr44 and Val45 in our sequence), Leu63, Arg70, and Asn74 form a large interaction area. It should be noted that we did not observe any NOEs between Asn74 and Thr44, or Val45 and Leu63.

There is also evidence for ephrin-induced phosphorylation of the conserved tyrosine in the EphB1 receptor SAM domain (Stein et al., 1996), leading to the subsequent binding of an SH2 domain from the adaptor protein Grb10. Our structure shows this tyrosine to be within the interior of the structure and a phosphorylation of this residue would require a conformational change whereby the hydrogen bond between the hydroxyl group of the tyrosine and the aromatic ring of His58 has to be broken. The presence of this hydrogen bond is probably also important for the stability of the fold, as the tyrosine and the histidine are usually pairwise conserved. The sequences of the EphA3 receptor SAM domains, for example, lack both at the same time. For this reason, it is also possible that the mutation Y929F in the EphB1 receptor (Stein et al., 1996) was responsible for destabilizing the protein.

In our EphB2 SAM solution structure, the conserved hydrophobic residue Leu55 buries the hydrogen bond between Tyr25 and

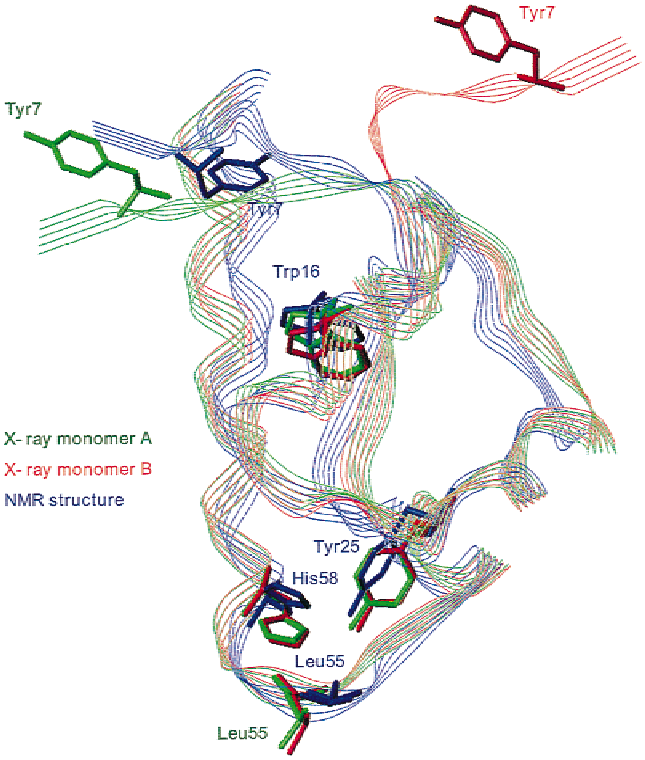

Fig. 3. Comparison of the EphB2 SAM domain solution structure (blue) with the two types of monomers from the oligomeric crystal structure (Thanos et al., 1999) (A, green; B, red). The N-terminus and C-terminal helix 5 are close together in the solution structure. The X-ray structure shows an open form with an exposed Tyr7. The pairwise conserved Tyr25 and His58 are involved in a hydrogen bond shielded by the hydrophobic Leu55. These residues are more solvent accessible in the crystal structure. The figure was created with SYBYL 6.4b (Tripos Inc.).

His58 making the hydroxyl group of Tyr25 poorly accessible for phosphorylation. This structural feature is well-defined by a number of characteristic NOEs. In contrast, Tyr25, Leu55 and His58 are not as closely packed and more solvent accessible in the oligomeric crystal structure (see Fig. 3). This structural difference may be caused by a conformational change in the event of oligomerization. This could also be a reason for the strong chemical shift changes in this area upon increasing protein concentration (Fig. 2C, area 2; Fig. 3). After receptor oligomerization, Tyr25 of the SAM domain may then become more accessible for a subsequent phosphorylation process.

A comparison of the interaction sites observed in the EphA4 and EphB2 crystal structures (Stapleton et al., 1999; Thanos et al., 1999) and the results of our chemical shift studies shows some similarities but also differences. One of the NMR-derived surfaces

Fig. 2 (*facing page*)**.** Structure of the SAM domain from the EphB2 receptor (stereo view). **A:** Superposition of the C′, N, Cα of eight NMR structures with the lowest energy including the side chains of residues in the hydrophobic core of the protein. **B:** Schematic representation of the SAM structure, showing the five helices in red/yellow and the side chains of Tyr25, His58, and Leu55 are marked in blue. The figure was created with MOLMOL (Koradi et al., 1996). **C:** Residues whose chemical shift changes show the strongest concentration dependency (area 1: Tyr7, Thr8, Phe10, Ala32, Asp38, Ile39, Asp47, Met69, and Met73, and area 2: Leu55, Ala56, Gly57, His58, Lys60, and Lys61) are presented with Conolly surfaces. Figures 2A and 2C were prepared with SYBYL 6.4b (Tripos Inc., St. Louis, Missouri).

involves residues at the N- and C-terminus (Tyr7, Phe10, Met69, Met73) (Fig. 2C, area 1). This interaction area is consistent with interfaces between monomers in the crystal structures of the EphA4 and EphB2 SAM domains. In the NMR investigation, this area is extended by the residues Ala32 and Asp47 (Fig. 2C, area 1), which is different to both X-ray structures. Thanos et al. (1999) show also a second set of crystal contacts including the surface of helix 5 and Met45 of their sequence. We do not observe stronger chemical shift changes in this area. The second NMR-derived surface involves residues Leu55, Ala56, Gly57, His58, Lys60, and Lys61 (Fig. 2C, area 2). This area does not participate in protein–protein contacts in the crystal structures. There are two possible explanations for this observation. There is still the possibility of subtle structural long-range effects caused by oligomerization. Alternatively, it can be assumed that this second site is used upon formation of tetramers or other higher oligomers. Interestingly, the surface exposed residues in area 2 are highly conserved. The tetramerization process of the EphB2 SAM domain may create new interfaces, providing an appropriate contact area for the binding of an LMW-PTP and the initiation of further downstream responses.

Materials and methods

Protein expression and purification

DNA sequences encoding the desired constructs of the SAM domain as shown in Figure 1 were PCR-amplified from chicken embryo kinase 5 cDNA. In each case the PCR product was purified and ligated into a pET28d vector for transformation of the *Escherichia coli* BL21(DE3) strain. Sequencing with standard ABI automated sequencer confirmed the identity of the insert. The clones were grown in LB medium containing 34 μg/mL chloramphenicol and 25 μg/mL kanamycin. Expression was induced at an OD_{600} with 1 mM IPTG. The cells were incubated for 4 h at 37 °C. All following procedures were carried out at 0–4 °C and were monitored using SDS-PAGE. The cell pellets were resuspended in lysis buffer (20 mM Tris-HCL pH 8.0, 1 mM PMSF) and lysed with a French press. The lysate was centrifuged and the supernatant was loaded onto a chelating sepharose column FF (Pharmacia, Uppsala, Sweden) equilibrated with buffer (20 mM Tris-HCL pH 8.0, 50 mM NaCL, 0,05% NaN_3). The protein was eluted using a step gradient of imidazole. The pooled fractions containing the protein were concentrated and further purified by gel filtration on a Superdex 75 column (Pharmacia). The purity of the protein was monitored by SDS-PAGE and mass spectroscopy. Uniformly $^{13}C/^{15}N$-labeled SAM protein was prepared for the NMR experiments by growing *E. coli* BL21(DE3) strain harboring the expression plasmid in a M9 minimal medium containing $^{15}NH_4Cl$, U-[$^{13}C_6$]glucose and 5% $^{13}C/^{15}N$-labeled Celtone (Martek, Columbia, Maryland). The protein was purified as described above. For the NMR measurements a buffer containing 20 mM KH_2PO_4/K_2HPO_4 at pH 5.8 or 7.4, 50 mM KCl, 0.05% NaN_3 was used. The protein concentrations varied between 0.1 and 3.0 mM. Depending on the necessities, samples in either in 90% H_2O/10% D_2O or 100% D_2O were prepared.

Protein characterization

Sedimentation equilibrium analysis of the SAM domain was performed using a Beckman XL-I analytical ultracentrifuge operating at 25.000 rpm and 300 K. The samples contained 80 μM and 1.6 mM protein in the same buffer as described above. NaN_3 was omitted for these measurements. Protein stability was measured with 40 μM protein solution in the pH range 5.8–8.0 using a Jasco J-720 spectropolarimeter to monitor the typical minima for α-helical proteins at 208 and 222 nm as a function of the temperature. Circular dichroism spectra were recorded between 10–80 °C with a step gradient of 10 °C.

NMR spectroscopy

All NMR experiments were recorded at 300K on Bruker DRX600 and DMX750 spectrometers, in standard configuration, using a [^{1}H, ^{13}C, ^{15}N] triple-resonance probe equipped with three axes, self-shielded gradient coils. The NMR spectra were processed with XWIN-NMR (Bruker Analytik GmbH, Rheinstetten, Germany). The data were analyzed using the programs AURELIA (Bruker Analytik GmbH) and ANSIG (Kraulis, 1989).

Homonuclear two-dimensional spectra NOESY (Jeener et al., 1979), TOCSY (Braunschweiler & Ernst, 1983) with DIPSI2-rc mixing (Cavanagh & Rance, 1992), and DQF-COSY (Piantini et al., 1982) were recorded using the unlabeled sample in 90% H_2O/10% D_2O, as well as 100% D_2O. NOESY spectra were recorded with mixing times of 20, 40, 80, and 120 ms. Heteronuclear multidimensional spectra were recorded with a sample of the double labeled protein. For the assignment of resonances, CBCA(CO)NNH (Grzesiek & Bax, 1992a), CBCANNH (Grzesiek & Bax, 1992b), HBHA(CBCACO)NNH (Grzesiek & Bax, 1993), and H(CCO)NNH-TOCSY (Montelione et al., 1992) were recorded in 90% H_2O/10% D_2O. HCCH-COSY (Kay et al., 1990) and HCCH-TOCSY (Bax et al., 1990) were recorded using 100% D_2O as solvent. A complete assignment of all resonances could be achieved. For the extraction of distance information, a ^{15}N-NOESY-HSQC (Clore & Gronenborn, 1991) was recorded using 90% H_2O/10% D_2O as solvent, and a ^{13}C-NOESY-HSQC (Clore & Gronenborn, 1991) using D_2O. NH-exchange rates were estimated from a set of MEXICO experiments (Gemmecker et al., 1993).

Structure calculation

The structures were calculated with the program X-PLOR (version 3.1) (Brünger, 1992) using the simulated annealing (SA) protocol (Nilges et al., 1988). Distance constraints were categorized as strong (1.8–2.8 Å), medium (1.8–3.5 Å), weak (1.8–5.0 Å), or very weak (2.5–6.0 Å). As pseudo-atom corrections 0.4 Å was added for equivalent methyl protons, 1.5 Å for the six equivalent methyl group protons in Leu and Val, and 2 Å for equivalent aromatic ring protons in Phe and Tyr (Fletcher et al., 1996). Distinguishable geminal methyl groups in Leu and Val and distinguishable prochiral methylene protons in the side chains were systematically selected during the SA using the floating assignment protocol. Hydrogen bond constraints were obtained for helices 1, 2, 4, and 5, by analyzing NH-exchange rates estimated from a set of MEXICO experiments (Gemmecker et al., 1993) and were allowed to full-fill both $i + 3$ and $i + 4$ hydrogen bond geometry.

Accession number

The coordinates of the solution structure of the SAM domain from the receptor tyrosine kinase EphB2 have been deposited in the PDB with the accession code 1sgg.

Acknowledgments

We thank G. Richter and A. Bacher, Technical University Munich, for analytical ultracentrifugation, E. Krause for mass spectroscopy, and L. Handel and M. Leidert for technical support. K. Kullander and R. Klein (EMBL Heidelberg) are kindly acknowledged for their attempts to phosphorylate SAM and R. Poppe (University of Mainz) for two-hybrid experiments.

References

Barr MM, Tu L, Van Aelst L, Wigler M. 1996. Identification of Ste4 as a potential regulator of Byr2 in the sexual response pathway of *Schizosaccharomyces pombe*. *Mol Cell Biol 16*:5597–5603.

Bax A, Clore GM, Gronenborn AM. 1990. ^{1}H-^{1}H correlation via isotropic mixing of ^{13}C magnetization, a new three-dimensional approach for assigning ^{1}H and 13C spectra of 13C enriched proteins. *J Magn Reson 88*:425–431.

Bork P, Koonin EV. 1998. Predicting functions from protein sequences—where are the bottlenecks. *Nature Genet 18*:313–318.

Braunschweiler L, Ernst RR. 1983. Coherence transfer by isotropic mixing: Application to proton correlation spectroscopy. *J Magn Reson 53*:521–528.

Brückner K, Pasquale EB, Klein R. 1997. Tyrosine phosphorylation of transmembrane ligands for Eph receptors. *Science 275*:1640–1643.

Brünger T. 1992. *X-PLOR version 3.1. A system for X-ray crystallography and NMR*. New Haven, Connecticut: Yale University Press.

Cavanagh J, Rance M. 1992. Suppression of cross-relaxation effects in TOCSY spectra via a modified DIPSI-2 mixing sequence. *J Magn Reson 96*:670–678.

Clore GM, Gronenborn AM. 1991. Application of three- and four-dimensional heteronuclear NMR spectroscopy to protein structure determination. *Prog NMR Spectrosc 23*:43–92.

Davis S, Gale NW, Aldrich TH, Maisonpierre PC, Lhotak V, Pawson T, Goldfarb M, Yancopoulos GD. 1994. Ligands for Eph-related receptor tyrosine kinases that require membrane attachment or clustering for activity. *Science 266*:816–819.

Eph Nomenclature Committee. 1997. *Cell 90*:403.

Fletcher CM, Jones DNM, Diamond R, Neuhaus D. 1996. Treatment of NOE constraints involving equivalent or nonstereoassigned protons in calculations of biomacromolecular structures. *J Biomol NMR 8*:292–310.

Gemmecker G, Jahnke W, Kessler H. 1993. MEXICO: Measurement of proton exchange rates in isotropically labeled compounds. *J Am Chem Soc 115*: 11620–11621.

Grzesiek S, Bax A. 1992a. Correlating backbone amide and side chain resonances in large proteins by multiple relay triple resonance NMR. *J Am Chem Soc 114*:6291–6293.

Grzesiek S, Bax A. 1992b. An efficient experiment for sequential backbone assignment of medium sized isotopically enriched proteins. *J Magn Reson 99*:201–207.

Grzesiek S, Bax A. 1993. Amino acid type determination in the sequential assignment procedure of uniformly $^{13}C/^{15}N$ enriched proteins. *J Biomol NMR 3*:185–204.

Holland SJ, Gale NW, Mbamalu G, Yancopoulos GD, Henkemeyer M, Pawson T. 1996. Bidirectional signaling through the Eph-family receptor Nuk and its transmembrane ligands. *Nature 383*:722–725.

Holm L, Sander C. 1993. Protein structure comparison by alignment of distance matrices. *J Mol Biol 233*:123–138.

Jeener J, Meier BH, Bachmann P, Ernst RR. 1979. Investigation of exchange processes by two-dimensional NMR spectroscopy. *J Chem Phys 71*:4546–4553.

Kay LE, Ikura M, Bax A. 1990. Proton-proton correlation via carbon-carbon couplings: A three-dimensional NMR approach for the assignment of aliphatic resonances in proteins labeled with carbon-13. *J Am Chem Soc 112*:888–889.

Koradi R, Billeter M, Wüthrich K. 1996. MOLMOL: A program for display and analysis of macromolecular structures. *J Mol Graphics 14*:51–55.

Kraulis P. 1989. ANSIG: A program for the assignment of protein ^{1}H two-dimensional NMR spectra by interactive computer graphics. *J Magn Reson 84*:627–633.

Kuo C-F, McRee DE, Fisher CL, O'Handley SF, Cunningham RP, Tainer JA. 1992. Atomic structure of the DNA repair [4Fe-4S] enzyme endonuclease III. *Science 258*:435–441.

Kyba M, Brock HW. 1998. The SAM domain of polyhomeotic, RAE28, and Scm mediates specific interactions through conserved residues. *Dev Genet 22*:74–84.

Laskowski RA, MacArthur MW, Moss DS, Thornton JM. 1993. PROCHECK: A program to check the stereochemical quality of protein structures. *J Appl Crystallogr 26*:283–291.

Montelione GT, Lyons BA, Emerson SD, Tashiro M. 1992. An efficient triple resonance experiment using carbon-13 isotropic mixing for the determining sequence-specific resonance assignment of isotropically-enriched proteins. *J Am Chem Soc 114*:6291–6293.

Murzin AG, Brenner SE, Hubbard T, Cottina C. 1995. SCOP: A structural classification of proteins database for the investigation of sequence and structures. *J Mol Biol 247*:536–540.

Nilges M, Gronenborn AM, Clore GM. 1988. Determination of three-dimensional structures of proteins from interproton distance data by hybrid distance-dynamical simulated annealing calculations. *FEBS Lett 239*:129–136.

Orioli D, Klein R. 1997. The Eph receptor family: Axonal guidance by contact repulsion. *Trends Genet 13*:354–359.

Piantini U, Sørensen DW, Ernst RR. 1982. Multiple quantum filter for elucidating NMR coupling networks. *J Am Chem Soc 104*:6800–6801.

Ponting CP. 1995. SAM: A novel motif in yeast sterile and *Drosophila* polyhomeotic proteins. *Protein Sci 4*:1928–1930.

Rafferty JB, Sedelnikova SE, Hargreaves D, Artymiuk PJ, Baker PJ, Sharples GJ, Mahdi AA, Lloyd RG, Rice DW. 1996. Crystal structure of DNA recombination protein RuvA and a model for its binding to the holliday junction. *Science 274*:415–421.

Sawaya MR, Pelletier H, Kumar A, Wilson SH, Kraut J. 1994. Crystal structure of a rat DNA polymerase b: Evidence for a common polymerase mechanism. *Science 264*:1930–1935.

Schultz J, Ponting CP, Hofmann K, Bork P. 1997. SAM as a protein interaction domain involved in developmental regulation. *Protein Sci 6*:249–253.

Stapleton D, Balan I, Pawson T, Sicheri F. 1999 The crystal structure of an Eph receptor SAM domain reveals a mechanism for modular dimerization. *Nature Struct Biol 6*:44–49.

Stein E, Cerretti DP, Daniel TO. 1996. Ligand activation of ELK receptor tyrosine kinase promotes its association with Grb10 and Grb2 in vascular endothelial cells. *J Biol Chem 271*:23588–23593.

Stein E, Lane AA, Cerretti DP, Schoecklmann HO, Schroff AD, Van Etten RL, Daniel TO. 1998. Eph receptors discriminate specific ligand oligomers to determine alternative signaling complexes, attachment, and assembly responses. *Genes Dev 12*:667–678.

Thanos CD, Goodwill KE, Bowie JU. 1999. Oligomeric structure of the human EphB2 receptor SAM Domain. *Science 283*:833–836.